SCIENTIFIC REPORTS

RETRACTED

OPEN

SUBJECT AREAS:
QUANTUM INFORMATION
INFORMATION TECHNOLOGY
QUANTUM OPTICS

Received
22 November 2013

Accepted
18 March 2014

Published
2 April 2014

Correspondence and requests for materials should be addressed to M.-X.L. (mxluo@home.swjtu.edu.cn) or G.X. (gangxu_bupt@163.com)

Efficient Quantum Transmission in Multiple-Source Networks

Ming-Xing Luo[1,2,3], Gang Xu[2,4], Xiu-Bo Chen[2], Yi-Xian Yang[2] & Xiaojun Wang[5]

[1]Information Security and National Computing Grid Laboratory, Southwest Jiaotong University, Chengdu 610031, China, [2]State Key Laboratory of Networking and Switching Technology, Beijing University of Posts and Telecommunications, Beijing 100876, China, [3]State Key Laboratory of Information Security (Graduate University of Chinese Academy of Sciences), Beijing 100049, China, [4]School of Software Engineering, Beijing University of Posts and Telecommunications, Beijing 100876, China, [5]School of Electronic Engineering, Dublin City University, Dublin 9, Ireland.

A difficult problem in quantum network communications is how to efficiently transmit quantum information over large-scale networks with common channels. We propose a solution by developing a quantum encoding approach. Different quantum states are encoded into a coherent superposition state using quantum linear optics. The transmission congestion in the common channel may be avoided by transmitting the superposition state. For further decoding and continued transmission, special phase transformations are applied to incoming quantum states using phase shifters such that decoders can distinguish outgoing quantum states. These phase shifters may be precisely controlled using classical chaos synchronization via additional classical channels. Based on this design and the reduction of multiple-source network under the assumption of restricted maximum-flow, the optimal scheme is proposed for specially quantized multiple-source network. In comparison with previous schemes, our scheme can greatly increase the transmission efficiency.

Maximizing information transmission is very important concern when dealing with limited-resource scenarios in large-scale networks. Network coding[1], which allows multiple messages to be encoded before transmission in common channels, may provide a solution for single-source networks. One typical example is illustrated in Figure 1(a). With linear encoding, the source node can simultaneously transmit two messages to all receivers from two edge-disjoint paths[1], even if two receivers share one common channel *CD*. The key is that two incoming messages $\{x, y\}$ are encoded into a new message $x + y$, at the node *C*. Each receiver can recover $\{x, y\}$ using $\{x, x + y\}$ or $\{y, x + y\}$. This task cannot be successfully performed using the trivial transmission scheme [store-forward routing for each node[2]] because in this scheme, only one message, x or y, may be transmitted in the common channel *CD* each time. Generally, transmission conflicts in common channels [network congestion] become serious problems [congestion collapse] in large-scale networks [Internet][3]. Fortunately, network coding can achieve the optimal Shannon capacity of single-source networks[1,2]. Network coding is considered to be an important technology for next-generation communication to achieve network multicasts[4–6] [*the sender simultaneously sends multiple messages to all receivers on a single-source network*] or *k*-pair transmissions[7,8], i.e., multiple unitcasts [*each sender transmits messages to its corresponding receiver simultaneously over multiple-source networks*].

When classical networks are quantized with quantum nodes and quantum channels, one may wish to optimize the transmission efficiency over large-scale quantum networks, as illustrated in Figure 1(b). Because of the quantum no-cloning theorem, the source node *O* may be replaced with two source nodes S_1 and S_2. Thus, the multicast over the Butterfly network is reduced to the 2-pair problem on the reduced quantum network with common channels[9]. However, perfect quantum *k*-pair transmissions have been proved to be impossible in the absence of any additional resources[10–12]. They require all incoming states $|\phi_i\rangle$ be encoded into a coherent superposition $\Sigma_i\, \alpha|\phi_i\rangle$ at the node *C*, and decoded at the node *D*. This is a rather difficult task. The situation may be changed if classical communications are freely allowed[13,14]. This assumption is reasonable because classical communications are much cheaper and more readily available than quantum communications. These results are dependent on the linear encodings[14] or the nonlinear encodings[15] applied in the enlarged encoding space, and give rise to three natural questions. The first question (Q1) is whether the enlarged encoding space is necessary for large-scale quantum network communications. The second question (Q2) is what amount of classical communication is sufficient. Classical two-way unlimited channels have been assumed to exist between any two nodes[14] or only between two quantum nodes connected by quantum channels[15]. The third question (Q3)

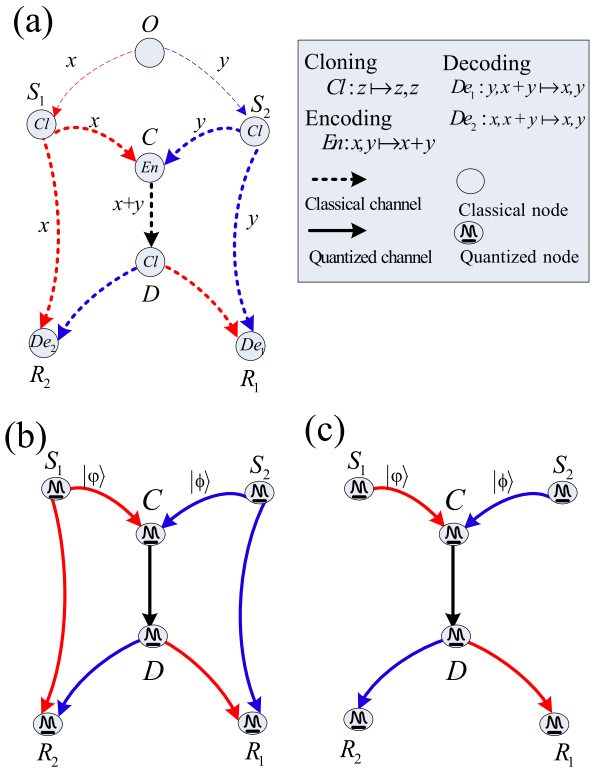

Figure 1 | Schematic network transmission over the Buttery network. (a) The classical network multicast with network coding. Each channel has unit transmission capacity. Each node R_i has two edge-disjoint paths originating from the source node O, $i = 1, 2$. CD is a common channel for two receivers. The input messages $\{x, y\}$ are encoded into $x + y$ at the node C, and forwarded to the node D. $x + y$ is copied [unit fidelity], and each message is forwarded to one node R_i. Each receiver can recover $\{x, y\}$ from $\{x, x + y\}$ or $\{y, x + y\}$. (b) The quantized network without the node O. All nodes and channels may be quantized with quantum participants and quantum channels, respectively. The node O is canceled because of the quantum no-cloning theorem at the node S_i. Thus, the quantum task is for each S_i to multicast an unknown state to all receivers simultaneously. (c) The reduced quantized network. The transmissions over the channels S_1R_2 and S_2R_1 are trivial and reduced. The remaining task is to design the transmission over the common channel CD.

is whether the linear encoding is sufficient for large-scale quantum network communications. These problems are related to the optimization of the transmission capacity of multiple-source quantum networks.

In this paper, based on the achievements of quantum information theory[16–20] and quantum networking theory[21–33], we investigate these problems using similar ideas in classical network coding. Unlike the entanglement quantization of a classical channel[9–16], it may be quantized with a continuous physical channel[26–36], and the transmission information may be quantized with quantized electromagnetic fields of identical frequencies. To distinguish the decoded quantum states for different nodes, special phase-shift operations may be designed to index different incoming quantum states, using phase shifters [coupling the optical fields to driven Duffing oscillators] or gauge transformations[33]. This encoding can spread the spectral content of the quantum information across the entire spectrum in order to encode the information, and can distinguish different senders with their own phase factors. Unfortunately, the added phase information is not easily decoded, and doing so requires the ability to precisely control the remote chaotic systems during the communication. To solve this problem, free classical communications are assumed between two quantum nodes with common channels, and are used to synchronize the remote phase shifters. This is classical chaos synchronization and may be achieved using the nonlinear coupling between the optical fields and Duffing oscillators[37–40] or semiconductor lasers[41–44]. The key is the nonlinear Kerr interaction, which can be used to couple the classical chaotic light with the information-bearing quantum light[45]. Recently, electrooptic modulators (EOMs) have also been used for chaos synchronization[46–48]. Moreover, all encoded quantum information may be combined into a coherent superposition state, and decoded using paired multiport beam splitters[49–51]. Based on our transmission schemes in common channels, using the network reduction shown in the supplementary information (SI), we can identify the optimal transmission scheme for quantum multiple-source networks assuming restricted maximum-flow. Our scheme is beyond both the quantum k-pair transmissions[13–15] based on the classical solvability and classical network transmissions[52–54] via network coding. These results may be beneficial for large-scale quantum network communications.

Results

Consider an acyclic directed quantized network $G_q = (\mathcal{V}_q, \mathcal{E}_q)$, as shown in Figure 2(a)). $\mathcal{V}_q$ and $\mathcal{E}_q$ are the node set and the edge set, respectively. Each node in $\mathcal{V}_q$ is quantized with a quantum participant that can perform all quantum operations and classical operations. The transmission information is quantized with electromagnetic fields a_j and b_j of the same frequency. Each channel in $\mathcal{E}_q$ is quantized with a continuous-time physical channel and has a unit transmission rate [one quantum state]. Each pair (S_i, R_j) has $l_{ij} \geq 1$ edge-disjoint paths. Our task is to allow efficient transmissions in large-scale quantum networks: All source-sink nodes pairs communicate simultaneously, subject to restricted maximum-flow. Although quantum multiple-source networks have no uniform network topology, based on the network reduction shown in the SI, the optimal quantum multiple-source transmission may be reduced to the transmission in the primitive network, as shown in Figure 2(b). Thus, special encoding and decoding operations should be designed to be suitable to the quantum task.

Restricted maximum-flow. In the optimization theory, the maximum-flow problem [unit capacity for each channel] is equivalent to identifying the maximal number of edge-disjoint paths between the source and the sink, under the assumption unit capacity of per edge. Our interest is in the case of restricted maximum-flow, i.e., no common channels for different source-sink node pairs are outgoing edges of source nodes or incoming edges of sink nodes. This assumption is reasonable because of the quantum non-cloning theorem.

Motivated by network coding[1–6] and quantum network theory[21–33], a schematic illustration of quantum transmission over a common channel is presented in Figure 3. The information-bearing field a_j originating from the node A_j is first shifted at the node C using a chaotic phase shifter (CPS_j) with the Hamiltonian $\delta_j(t)a_j^\dagger a_j$ and the time-dependent classical chaotic signal $\delta_j(t)$, $j = 1, \cdots, n$. This phase shift corresponds to the gauge transformation in the nearest nodes[30]. All new quantum information is encoded using a multiport beam splitter (MBS_1), and transmitted over the common channel CD. The combined quantum information is amplified using a phase-insensitive linear amplifier (LA) at the node D to compensate for the information losses induced by MBS_1, and then decomposed into n different components by MBS_2. The amplifier gain of the LA is $n + 1$. All decomposed information may be decoded using CPS'_j [the inverse of CPS_j] with the corresponding Hamiltonian $-\delta'_j(t)b_j^\dagger b_j$, $j = 1, \cdots, n$. Each decoded information-bearing field b_j is sent to the subsequent node B_j, $j = 1, \cdots, B_n$.

Note that each pair of CPS_j and CPS'_j induces phase shifts with the phase $\exp(i\theta_j(t))$ and the inverse phase $\exp(-i\theta_j(t))$, respectively,

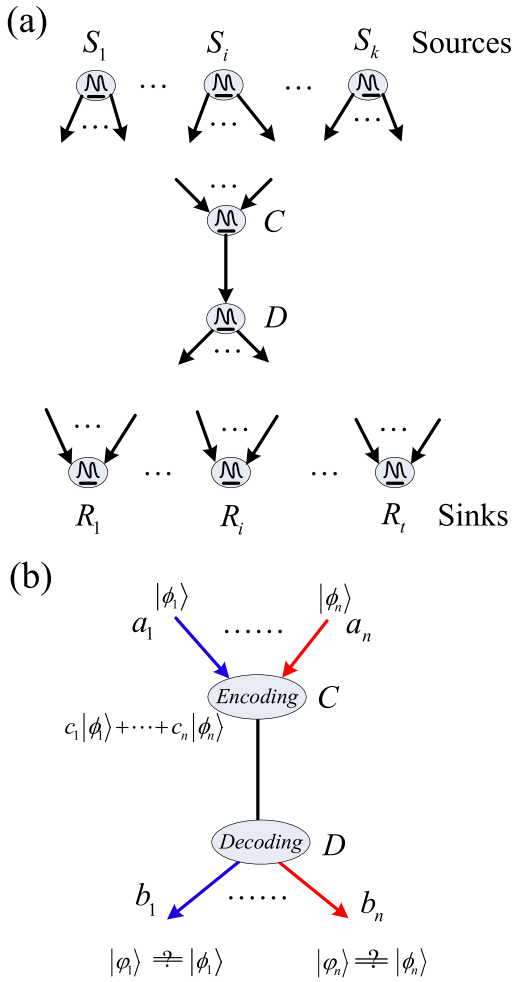

Figure 2 | Schematic acyclic directed quantum multiple-source network. (a) $\{S_1,\cdots S_k\}$, $\{R_1,\cdots,R_t\}\subset\mathcal{V}$ are source and target nodes, respectively. Each pair S_iR_j has l_{ij} edge-disjoint paths. CD is a common channel for different pairs. No common channel is the outgoing edge of a source node or the incoming edge of a sink node. (b) The primitive subnetwork of quantum multiple-source networks. a_j and b_j are information-bearing fields of quantum information [the original fields generated by the former nodes]. The node C has n incoming edges, and the node D has n outgoing edges. The transmission in the channel CD is the main concern for quantum multiple-source transmission tasks. All incoming states $|\phi_1\rangle,\cdots,|\phi_n\rangle$ should be encoded into a superposition state at the node C, and decoded at the node D.

where $\theta_j(t)=\int_0^t\delta_j(\tau)d\tau$. To achieve faithful transmission, these transformations must be precisely controlled during the process of quantum communication, i.e., it must be ensured that the two chaotic systems have the same parameters, initial values, and evolutions such that $\delta_j(t)=\delta_j'(t)$ for each $j=1,\cdots,n$. However, this precise control is impractical for remote participants because the chaotic system is unstable in system parameters and initial values. Therefore, additional classical channels are assumed to exist for common channel CD, and used to synchronize each pair of CPS_j and CPS_j', $j=1,\cdots,n$, as shown in Figure 3(b). These classical channels are cheap and readily available compared with quantum channels.

Modeling quantum transmission over a common channel. Consider the primitive quantum network shown in Figure 3(b). Each pair of CPS_j and CPS_j' has been synchronized prior to the transmission of

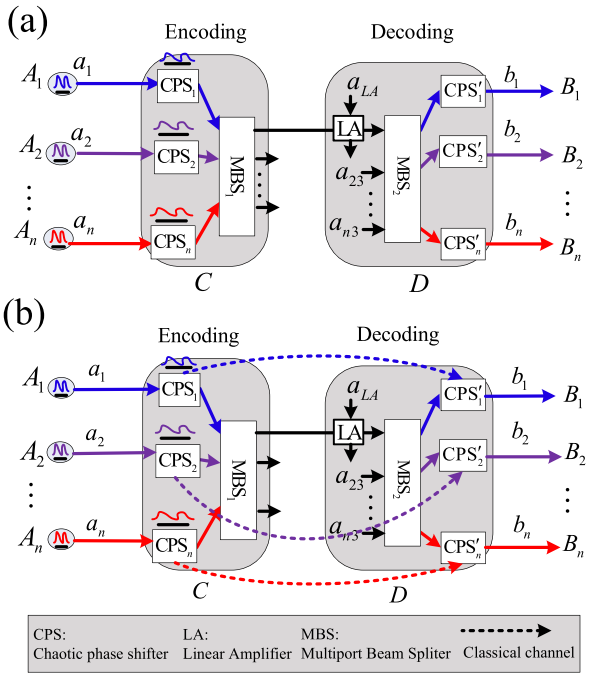

Figure 3 | Schematic quantum transmission over a common channel. (a) Quantum transmission without additional classical channels. $a_{LA}^{\dagger}$ is the creation operator of the auxiliary vacuum field entering the LA, and a_{j3} denotes the annihilation operator entering the second MBS (MBS_2), $j=1,\cdots,n$. The encoding at the node C is performed using CPS_j and MBS_1. The decoding at the node D is performed using the LA, MBS_2 and CPS_j' [the inverse of CPS_j]. (b) Quantum transmission with additional classical channels for the common channel. The encoding is identical to that shown in Figure 3(a)), whereas the decoding is performed using the chaotic synchronization of CPS_j and CPS_j', $j=1,\cdots,n$.

quantum information, $j=1,\cdots,n$. The information-bearing fields $a_1,\cdots,a_n$ with the same frequency ω_c are modulated using n different pseudo-noise signals and pass through CPS_j, MBS_1, the LA, MBS_2, and CPS_j' sequentially. The global quantum transmission can be described using the following linear relation:

$$b_j=a_j+\frac{1}{n}\sum_{k=1,k\neq j}^{n}e^{i\left(\theta_j-\theta_k\right)_{a_k}}+\sum_{s=2}^{n}e^{i\theta_j}\beta_{js}a_{s3}+\sqrt{\frac{n^2-1}{n}}e^{i\theta_j}a_{LA}^{\dagger}\qquad(1)$$

for all $j=1,\cdots,n$. The matrices $(\alpha_{ij})_{n\times n}$ and $(\beta_{ij})_{n\times n}$ denote the transformations of MBS_1 and MBS_2, respectively, and satisfy $\lambda\alpha_{11}\beta_{11}=\cdots=\lambda\alpha_{1n}\beta_{n1}=1$. a_{s3} denotes the annihilation operator of the auxiliary vacuum field entering MBS_2, $s=2,\cdots,n$. For the pseudo-noise chaotic phase shift $\theta_j(t)$ from the CPSs, one needs to take an average over the broadband random signal, i.e., $\overline{\exp\left(\pm i\theta_j(t)\right)}\approx\sqrt{M_j}$, with $M_j=\exp\left(-\pi\int_{\omega_{lj}}^{\omega_{uj}}S_{\delta_j}(\omega)\Big/\omega^2d\omega\right)$ and the power-spectrum density $S_{\delta_j}(\omega)$ of signal $\delta_j(t)$. Here, ω_{lj} and ω_{uj} are the lower and upper frequency-band bounds of $\delta_j(t)$, respectively. Thus, the equation (1) is further reduced to

$$b_j=a_j+\frac{1}{n}\sum_{k=1,k\neq j}^{n}\sqrt{M_jM_k}a_k+\sum_{s=2}^{n}\sqrt{M_j}\beta_{js}a_{BS_s}+\sqrt{\frac{n^2-1}{n}}\sqrt{M_j}a_{LA}^{\dagger}.\qquad(2)$$

All M_j are extremely small with respect to the chaotic signal with the broadband frequency spectrum, and thus can be ignored in equation (2), therefore

$$b_j\approx a_j,\qquad(3)$$

i.e., faithful transmission of quantum information is achieved from the node A_j to the node A'_j, $j=1,\cdots,n$.

Quantum state transmission over a common channel. Consider pure qudit state transmission over the proposed model, as shown in Figure 4. The transmitted states are dark states of general Λ-type $d+1$-level atoms $\left|\phi_j\right\rangle=\sum_{i=0}^{d-1}\xi_{ij}|i\rangle_j$ with $\xi_{ij}\in[0,1]$, where the j-th atom is located in the cavity CA_j [see Figure 4(a)], $j=1,\cdots,n$. These states are transferred to the cavities via Raman transitions, transmitted over the quantum network, and stored in the new cavities. Assume that $2n$ coupled atom-cavity systems have the same parameters. By adiabatically eliminating the highest energy level $|d\rangle_j$, the atom j will always lie in the lowest d energy levels $|0\rangle_j,\cdots,|d-1\rangle_j$. The neighboring transition $|i\rangle_j\leftrightarrow|i+1\rangle_j$ is driven by a near-resonant laser field, and is coupled to the classical control field and the quantized cavity field with a coupling strength $\Omega_{ij}(t)$. The Hamiltonian of the atom-cavity systems can be expressed as

$$H_j=\sum_{i=0}^{d-1}g_{ij}(t)\left(c_j|i+1\rangle_j\langle i|+c_j^{\dagger}|i\rangle_j\langle i+1|\right), \tag{4}$$

where c_j is the annihilation operator of the j-th cavity mode; $g_{ij}(t)=g\Omega_{ij}(t)/\Delta$ is the coupling strength tuned by the classical control field

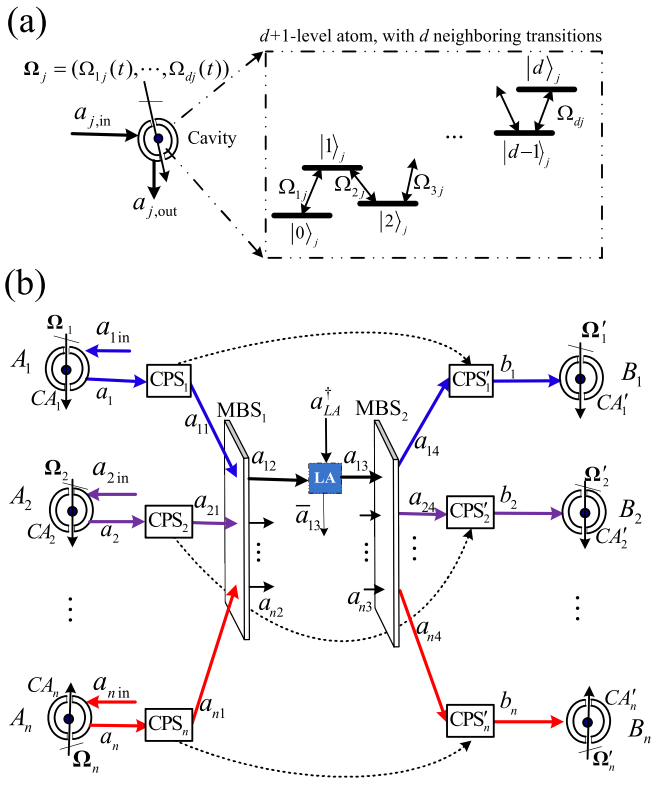

Figure 4 | Quantum state transmission over a common channel. (a) The circular symbols denote atom cavities. $\Omega_{ij}(t)$ denotes the amplitudes of classical driving fields in each cavity. Ω_{ij} denotes the transition frequency of $|i\rangle_j$ to $|i+1\rangle_j$. The circle in the center denotes a general Λ-type $d+1$-level atom. $a_{j\,in}$ [vacuum states] is the input field, $j=1,\cdots,n$. (b) Schematic quantum transmission over a common channel. $a_{j\,in}$ denotes the incoming information-bearing fields of nodes A_j, $j=1,\cdots,n$. a_{j1} and a_{j2} are the incoming and outgoing information-bearing fields of MBS_1, respectively; and a_{j3} and a_{j4} are the incoming and outgoing information-bearing fields of MBS_2, respectively, $j=1,\cdots,n$. $a^{\dagger}_{LA}$ and $\bar{a}_{13}$ are one of the incoming and outgoing information-bearing fields of the LA, respectively.

$\Omega_{ij}(t)$, $j=1,\cdots,n$; and Δ is the atom-cavity detuning. c_j is related to the traveling field a_j as follows:

$$a_j=\sqrt{\lambda}c_j+a_{j,in}, \tag{5}$$

$$a'_{j,out}=\sqrt{\lambda}c'_j+a'_j, \tag{6}$$

where λ is the decay rate of the cavity field.

CPS_j and CPS'_j are realized by coupling the optical fields to Duffing oscillators[37–44], as described by the Hamiltonian

$$H_{D,j}=\omega_0\pi\left(p_j^2+q_j^2\right)-\mu q_j^4-\gamma\cos(\omega_d t)q_j, \tag{7}$$

where p_j and q_j are the normalized position and momentum of the Duffing oscillators, respectively; ω_0 is the frequency of the fundamental mode; and μ, γ, and ω_d are constants. The interaction between the field a_j and Duffing oscillators is given by the Hamiltonian $\hat{H}_j=\zeta_j x_j a_j^{\dagger}a_j$, where ζ_j is the coupling strength between the field a_j and the oscillators. By choosing a suitable interaction, a phase factor $\exp\left(-i\int_0^t\zeta_j x_j(\tau)d\tau\right)$ can be generated for the field a_j. Moreover, the chaotic synchronization between CPS_j and CPS'_j may be achieved by using the harmonic potential coupling $V\left(x_j,x'_j\right)=\eta_j\left(x_j-x'_j\right)^2$, $j=1,\cdots,n$.

To show the quantum transmission efficiency, let us calculate the fidelity $F_j=\left\langle\phi_j\left|\rho'_j\right|\phi_j\right\rangle$, where ρ'_j is the quantum state received by the atom j'. From equation (2), the fidelity F_j can be approximated as 1 when $M\approx 0$, i.e., when Duffing oscillators enter the hard chaotic regimes[37–44]. This result means that qudit states can be faithfully transmitted over this primitive network via a common channel.

Quantum transmission in a multiple-source network. Note that according to the network reduction shown in the SI, the number of incoming channels for one common channel is equal to the number of outgoing channels. Thus, each common channel CD is equivalent to m distinct quantum channels $C_1D_1,\cdots,C_mD_m$ [not common channels] aided by additional classical channels, where m denotes the number of incoming channels, as shown in Figure 5. By replacing all common channels with equivalent quantum channels, an equivalent multiple-source network $\hat{G}_q=\left(\hat{\mathcal{V}}_q,\hat{\mathcal{E}}_q\right)$ can be constructed, which satisfies that all pairs (S_i,R_j) have no common channels under the assumption of restricted maximum-flow. Here, the source nodes and the sink nodes are unchanged. The resultant quantum transmission can be easily achieved via forward routing on the equivalent network with the aid of chaotic synchronization on the auxiliary classical channels. Thus, we identify and implement the optimal quantum transmission under the assumption of restricted maximum-flow in a multiple-source network, and partially answer the questions Q1–Q3. More specifically, the un-enlarged linear encoding [encoding operations such as those represented by equation (1)] is sufficient for large-scale quantum network communications under the assumption of restricted maximal-flow, and unlimited classical one-way channels corresponding to the common quantum channel are assumed. Of course, classical synchronization should be applied prior to the transmission in the common channel and requires some classical communication.

Discussion

We have introduced quantum multiple-source networks based on classical multiple-source networks and chaotic synchronization, where quantum information can be simultaneously transmitted in multiple subnetworks derived from source-sink node pairs. The proposed quantum transmission attains the optimal transmission

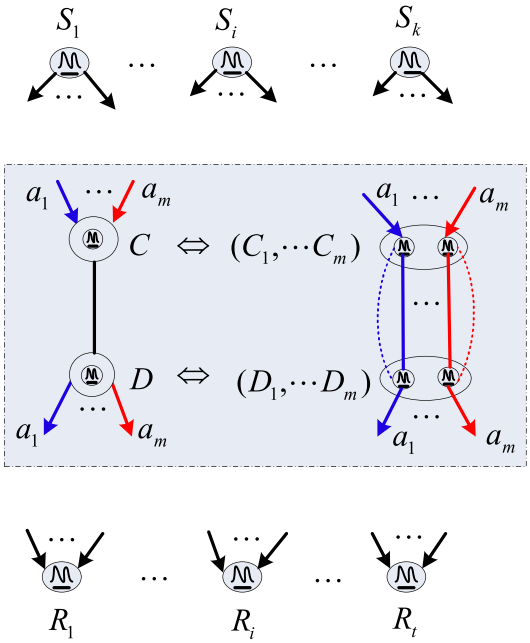

Figure 5 | Schematic illustration of quantum transmission in a multiple-source quantum network. $S_1, \cdots, S_k$ are source nodes, and $R_1, \cdots, R_t$ are sink nodes. The channel CD is a common channel for various source-sink node pairs. $C_1D_1, \cdots, C_mD_m$ are the equivalent m distinct quantum channels, supported by additional classical channels. m denotes the number of distinct quantum paths. All pairs (S_i, R_j) have no common channels in the equivalent network under the assumption of restricted maximum-flow.

capacity under the assumption of restricted maximum-flow; in this respect, it is superior to other proposed approaches[9–15]. Unlike quantum k-pair tasks with enlarged linear encodings[13,14] or nonlinear encodings[15], our encoding is linear and is not completed in an enlarged space. And classical channels are assumed to exist only for the common quantum channels and not all quantum channels[15]. Moreover, the new scheme extends the solvability of the quantum k-pair problem, and is more general than previous schemes[13–15] which depend on the solvability of the classical k-pair problem. One typical example is presented in the Figure 1(c); this example is unsolvable[52–54] in terms of the classical 2-pair problem using network coding. Other examples are provided in the SI. Our result is also different from continuous-time quantum walks[33], these examples break the time-reversal symmetry of the unitary dynamics for the purpose of enabling directional control, enhancement, and suppression of quantum transport. However, it requires controlling the chiral system for the gauge transformations, which may be difficult in case of remote systems in large-scale quantum networks. We use auxiliary classical channels to achieve similar transformations with the aid of chaotic synchronization. The proposed scheme can avoid to precisely controlling different chaotic phase shifts, and should be useful for large-scale quantum networks. Furthermore, the linear optical equipments are used to encode different quantum states and solve the transmission congestion on common channels. Generally, we can get the optimal transmission scheme in multiple-source network under the assumption of restricted maximum-flow. Of course, our proposal entails three important experimental requirements. The first one is the quantum interference of signals from different chaotic sources[55,56]. The second is the implementation of chaotic phase shifters and their synchronization, which may be achieved using all-optical systems[39] or optoelectronic[44]. The third is the implementation of multiport beam splitters[49–51]. More specifically, only the coefficients of the first column or row are relevant to our proposal; this feature may reduce the design complexity. These issues may not be far out of reach because of recent experimental and theoretical developments. Our schemes may provide one method for long-distance quantum network communications.

Methods

We calculate the linear mapping over the quantum network shown in the Figure 4(b). The mapping relationships of the $\mathrm{CPS}'_1, \cdots, \mathrm{CPS}'_n$ may be represented as

$$\begin{pmatrix} a_{11} \\ \vdots \\ a_{n1} \end{pmatrix} = \begin{pmatrix} e^{-i\theta_1} & & \\ & \ddots & \\ & & e^{-i\theta_n} \end{pmatrix} \begin{pmatrix} a_1 \\ \vdots \\ a_n \end{pmatrix}, \tag{8}$$

where a_{i1} and a_i are the annihilation operators of the auxiliary vacuum fields entering and output the CPS_i respectively, $i = 1, \cdots, n$. The mapping relationship of the MBS_1 is defined as

$$\begin{pmatrix} a_{12} \\ \vdots \\ a_{n2} \end{pmatrix} = \begin{pmatrix} \alpha_{11} & \cdots & \alpha_{1n} \\ \vdots & \ddots & \vdots \\ \alpha_{n1} & \cdots & \alpha_{nn} \end{pmatrix} \begin{pmatrix} a_{11} \\ \vdots \\ a_{n1} \end{pmatrix}, \tag{9}$$

where $a_{12}, \cdots, a_{n2}$ are the annihilation operators of the auxiliary vacuum fields entering the MBS_1. The mapping relationship of the LA is defined as

$$a_{13} = \lambda a_{12} + \sqrt{G - \lambda^2}\, a^{\dagger}_{LA}, \tag{10}$$

$$\bar{a}_{13} = \sqrt{G - \lambda^2}\, a^{\dagger}_{12} + \lambda a_{LA}, \tag{11}$$

where $a^{\dagger}_{LA}$ is the creation operator of the auxiliary vacuum field entering the LA. The mapping relationship of the MBS_2 is defined as

$$\begin{pmatrix} a_{14} \\ \vdots \\ a_{n4} \end{pmatrix} = \begin{pmatrix} \beta_{11} & \cdots & \beta_{1n} \\ \vdots & \ddots & \vdots \\ \beta_{n1} & \cdots & \beta_{nn} \end{pmatrix} \begin{pmatrix} a_{13} \\ \vdots \\ a_{n3} \end{pmatrix}, \tag{12}$$

where a_{i3} and a_{i4} are the annihilation operators of the auxiliary vacuum fields entering and outcoming the MBS_2 respectively, $i = 1, \cdots, n$. The mapping relationship of the $\mathrm{CPS}'_1, \cdots \mathrm{CPS}'_n$ are defined as

$$\begin{pmatrix} b_1 \\ \vdots \\ b_n \end{pmatrix} = \begin{pmatrix} e^{i\theta_1} & & \\ & \ddots & \\ & & e^{i\theta_n} \end{pmatrix} \begin{pmatrix} a_{14} \\ \vdots \\ a_{n4} \end{pmatrix}, \tag{13}$$

where b_j is the annihilation operator of the auxiliary vacuum field outcoming the CPS_j, $j = 1, \cdots, n$. Then, combining these equations and the conditions $\lambda = n$, $\alpha_{11} = \cdots = \alpha_{1n} = \beta_{11} = \cdots = \beta_{n1} = 1/\sqrt{n}$, the total input-output relationship of the quantum network is

$$b_j = a_j + \frac{1}{n}\sum_{k \neq j} e^{i(\theta_j - \theta_k)} a_k + \sum_{s=2}^{n} e^{i\theta_j} \beta_{js} a_{s3} + \sqrt{\frac{n^2 - 1}{n}} e^{i\theta_j} a^{\dagger}_{LA}, \tag{14}$$

where θ_j is independent chaotic noise, $j = 1, \cdots, n$.

Averaging the chaotic phase shift. The chaotic signal $\delta_j(t)$ may be expressed as a combination of many high-frequency components, i.e.,

$$\delta_j(t) = \sum_k A_{jk} \cos\left(\omega_{jk} t + \phi_{jk}\right), \tag{15}$$

where A_{jk}, ω_{jk}, ϕ_{jk} are the amplitude, frequency, and phase of each component, respectively. Then the phase of the signal is defined as

$$\theta_j(t) = \int_0^t \delta_j(\tau) d\tau = \sum_k \frac{A_{jk}}{\omega_{jk}} \left(\sin\left(\omega_{jk} t + \phi_{jk}\right) - \sin\left(\phi_{jk}\right)\right).$$

Using the Fourier-Bessel series identity[57] $\left[\exp(ix \sin y) = \sum_n J_n(x) \exp(iny)\right]$ with the n-th Bessel function of the first kind $J_n(x)$], we can write

$$\exp\left(-i\theta_j(t)\right) = \prod_k \left[\sum_{n_k} J_{n_k}\left(\frac{A_{jk}}{\omega_{jk}}\right) e^{-in_k\omega_{jk}t - in_k\phi_{jk} + i\sum_k \frac{A_{jk}}{\omega_{jk}} \sin\left(\phi_{jk}\right)}\right]. \tag{16}$$

Take average over the random phase ω_{ik}, the components related to the high-frequencies is averaged out because of the energy dissipation. It means that the resultant is only the near-resonance components, i.e, the lowest-frequency terms $[n_k = 0]$ dominating the dynamical evolution. Thus, we have

$$\overline{\exp\left(-i\theta_j(t)\right)} = \prod_k J_0\left(\frac{A_{jk}}{\omega_{jk}}\right) e^{i\sum_k \frac{A_{jk}}{\omega_{jk}} \sin\left(\phi_{jk}\right)}. \tag{17}$$

Moreover, since the chaotic signal $\delta_i(t)$ is mainly distributed in the high-frequency regime, we have $A_{jk} \ll \omega_{jk}$.

$$\overline{\exp(-i\theta_j(t))} \approx \prod_k J_0\left(\frac{A_{jk}}{\omega_{jk}}\right). \tag{18}$$

Using the approximations $J_0(x) \approx 1 - x^2/4$ and $\log(1 + x) \approx x$ for $x \ll 1$, it easily follows that

$$\begin{aligned}\prod_k J_0\left(\frac{A_{jk}}{\omega_{jk}}\right) &= \exp\left[\sum_k \log\ J_0\left(\frac{A_{jk}}{\omega_{jk}}\right)\right] \\ &\approx \exp\left(-\frac{1}{4}\sum_k \frac{A_{jk}^2}{\omega_{jk}^2}\right) \\ &= \exp\left(-\frac{\pi}{2}\int_{\omega_{ij}}^{\omega_{uj}} \frac{S_{\delta_j}(\omega)}{\omega^2} d\omega\right) \\ &= \sqrt{M_i},\end{aligned} \tag{19}$$

where $M_j = \exp\left(-\pi \int_{\omega_{ij}}^{\omega_{uj}} S_{\delta_j}(\omega)/\omega^2 d\omega\right)$.

Consequently, from equations (9) and (10), we obtain the approximation

$$\overline{\exp(-i\theta_j(t))} \approx \sqrt{M_j}. \tag{20}$$

1. Ahlswede, R., Cai, N., Li, S.-Y. R. & Yeung, R. W. Network information flow. *IEEE Trans. Inform. Theory* **46**, 1204–1216 (2000).
2. Gross, J. L. & Yellen, J. (ed.) [Network flows and applications] [534–573] (Chapman and Hall/CRC, 2005).
3. Floyd, S. & Fall, K. Promoting the use of end-to-end congestion control in the Internet. *IEEE/ACM Trans. Network.* **7**, 458–472 (1999).
4. Li, S.-Y. R., Yeung, R. W. & Cai, N. Linear network coding. *IEEE Trans. Inform. Theory* **49**, 371–381 (2003).
5. Tracey, H. *et al.* A random linear network coding approach to multicast. *IEEE Trans. Inform. Theory* **52**, 4413–4430 (2006).
6. Yeung, R. W., Li, S.-Y. R., Cai, N. & Zhang, Z. Network coding theory. *Found. Trends Commun. Inform. Theory* **2**, 241–381 (2005).
7. Fragouli, C. & Soljanin, E. Network coding fundamentals. *Found. Trends Net.* **2**, 1–133 (2007).
8. Leow, C. Y., Ding, Z., Leung, K. K. & Goeckel, D. L. On the study of analogue network coding for multi-pair, bidirectional relay channels. *IEEE Trans. Wireless Commun.* **10**, 670–681 (2011).
9. Hayashi, M., Iwama, K., Nishimura, H., Raymond, R. & Yamashita, S. Quantum network coding. arXiv:**0601088** (2006).
10. Hayashi, M. Prior entanglement between senders enables perfect quantum network coding with modification. *Phys. Rev. A* **76**, 040301 (2007).
11. Ma, S. Y., Chen, X. B., Luo, M. X., Niu, X. X. & Yang, Y. X. Probabilistic quantum network coding of *M*-qudit states over the butterfly network. *Opt. Commun.* **283**, 497–501 (2010).
12. Leung, D., Oppenheim, J. & Winter, A. Quantum network communication-the butterfly and beyond. *IEEE Trans. Inform. Theory* **6**, 3478–3490 (2010).
13. Kobayashi, H., Le Gall, F., Nishimura, H. & Röteler, M. General scheme for perfect quantum network coding with free classical communication. *LNCS* **5555**, 622–633 (2009).
14. Kobayashi, H., Le Gall, F., Nishimura, H. & Rötteler, M. Perfect quantum network communication protocol based on classical network coding. *Proceedings 2010 IEEE International Symposium on Information Theory (ISIT 2010)*, Austin, TX, USA; DOI:10.1109/ISIT.2010.5513644 (2010).
15. Kobayashi, H., Le Gall, F., Nishimura, H. & Röetteler, M. Constructing quantum network coding schemes from classical nonlinear protocols. *Proceedings 2011 IEEE In- ternational Symposium on Information Theory (ISIT 2011)*, Saint-Petersburg, Russia; DOI:10.1109/ISIT.2011.6033701 (2011).
16. Sangouard, N., Simon, C., Riedmatten, H. de. & Gisin, N. Quantum repeaters based on atomic ensembles and linear optics. *Rev. Mod. Phys.* **83**, 33–80 (2011).
17. You, J. Q. & Nori, F. Atomic physics and quantum optics using superconducting circuits. *Nature* **474**, 589–597 (2011).
18. Clarke, J. & Wilhelm, F. K. Quantum bits. *Nature* **453**, 1031–1042 (2008).
19. Chanelie, T., Matsukevich, D. N., Jenkins, S. D., Lan, S.-Y., Kennedy, T. A. B. & Kuzmich, A. Storage and retrieval of single photons transmitted between remote quantum memories. *Nature* **438**, 833–836 (2005).
20. Wang, X. B., Hiroshima, T., Tomita, A. & Hayashi, M. Quantum information with Gaussian states. *Phys. Rep.* **448**, 1–111 (2007).
21. Ritter, S. *et al.* An elementary quantum network of single atoms in optical cavities. *Nature* **484**, 195–200 (2012).
22. Chen, T.-Y. *et al.* Metropolitan all-pass and inter-city quantum communication network. *Opt. Exp.* **18**, 27217–27225 (2010).
23. Paparo, G. D. & Martin-Delgado, M. A. Google in a quantum network. *Sci. Rep.* **2**, 444 (2012).
24. Paparo, G. D., Mueller, M., Comellas, F. & Martin-Delgado, M. A. Quantum Google in a complex network. *Sci. Rep.* **3**, 2773 (2013).
25. Smith, G. & Yard, J. Quantum communication with zero-capacity channels. *Science* **321**, 1812–1815 (2008).
26. Czekaj, L. & Horodecki, P. Purely quantum superadditivity of classical capacities of quantum multiple access channels. *Phys. Rev. Lett.* **102**, 110505 (2009).
27. Zhang, J. *et al.* Quantum internet using code division multiple access. *Sci. Rep.* **3**, 2211 (2013).
28. Yoshino, K. *et al.* High-speed wavelength-division multiplexing quantum key distribution system. *Opt. Lett.* **37**, 223–225 (2012).
29. Brassard, G., Bussieres, F., Godbout, N. & Lacroix, S. Multiuser quantum key distribution using wavelength division multiplexing. *Proc. SPIE* **5260**, 149–153 (2003).
30. Kimble, H. J. The quantum internet. *Nature* **453**, 1023–1030 (2008).
31. Saglamyurek, E. *et al.* Broadband waveguide quantum memory for entangled photons. *Nature* **469**, 512–515 (2011).
32. Faccin, M., Johnson, T., Biamonte, J., Kais, S. & Migda l, P. Degree distribution in quantum walks on complex networks. *Phys. Rev. X* **3**, 041007 (2013).
33. Zimborás, Z., Faccin, M., Kádár, Z., Whitfield, J. D., Lanyon, B. P. & Biamonte, J. Quantum transport enhancement by time-reversal symmetry breaking. *Sci. Rep.* **3**, 2361 (2013).
34. Mülken, O. & Blumen, A. Continuous-time quantum walks: Models for coherent transport on complex networks. *Phys. Rep.* **502**, 37–87 (2011).
35. Klimov, A. B. & Chumakov, S. M. (ed.) [A group-theoretical approach to quantum optics: models of atom-field interactions] [45–69] (WILEY-VCH Verlag GmbH & Co. KGaA, 2009).
36. Landau, R. H. (ed.) [Quantum mechanics II: a second course in quantum theory] [309–323] (WTLEY-VCH Verlag GmbH & Co. KGaA 2007).
37. Shim, S.-B., Imboden, M. & Mohanty, P. Synchronized oscillation in coupled nanomechanical oscillators. *Science* **316**, 95–99 (2007).
38. Zhang, M., Wiederhecker, G. S., Manipatruni, S., Barnard, A., McEuen, P. & Lipson, M. Synchronization of micromechanical oscillators using light. *Phys. Rev. Lett.* **109**, 233906 (2012).
39. Manzano, G., Galve, F., Giorgi, G. L., Hernádez-García, E. & Zambrini, R. Synchronization, quantum correlations and entanglement in oscillator networks. *Sci. Rep.* **3**, 1439 (2013).
40. Ohtsubo, J. Chaos synchronization and chaotic signal masking in semiconductor lasers with optical feedback. *IEEE J. Quantum Electron.* **38**, 1141–1154 (2002).
41. Deng, T. *et al.* Chaos synchronization in mutually coupled semiconductor lasers with asymmetrical bias currents. *Opt. Exp.* **19**, 8762–8773 (2011).
42. Winkler, M., Butsch, S. & Kinzel, W. Pulsed chaos synchronization in networks with adaptive couplings. *Phys. Rev. E* **86**, 016203 (2012).
43. Reidler, I. Coupled lasers: phase versus chaos synchronization. *Opt. Lett.* **38**, 4174–4177 (2013).
44. Xiao, Y. F., Ozdemir, S. K., Gaddam, V., Dong, C. H., Imoto, N. & Yang, L. Quantum non-demolition measurement of photon number via optical Kerr effect in an ultra-high- microtoroid cavity. *Opt. Exp.* **16**, 21462 (2008).
45. Tsang, M. Cavity quantum electro-optics. II. Input-output relations between traveling optical and microwave fields. *Phys. Rev. A* **84**, 043845 (2011).
46. Williams, C. R. S. *et al.* Experimental observations of group synchrony in a system of chaotic optoelectronic oscillators. *Phys. Rev. Lett.* **110**, 064104 (2013).
47. Xiang, Z.-L., Ashhab, S., You, J. Q. & Nori, F. Hybrid quantum circuits: Superconducting circuits interacting with other quantum systems. *Rev. Mod. Phys.* **85**, 623–653 (2013).
48. Reck, M. & Zeilinger, A. Experimental realization of any discrete unitary operator. *Phys. Rev. Lett.* **73**, 58–61 (1994).
49. Törmä, P. & Jex, I. Plate beam splitters and symmetric multiports. *J. Modern Opt.* **43**, 2403–2408 (1996).
50. Peruzzo, A., Laing, A., Politi, A., Rudolph, T. & O'Brien, J. L. Multimode quantum interference of photons in multiport integrated devices. *Nature Commun.* **2**, 224 (2011).
51. Metcalf, B. J. *et al.* Multiphoton quantum interference in a multiport integrated photonic device. *Nature Commun.* **4**, 1356 (2013).
52. Dougherty, R., Freiling, C. F. & Zeger, K. Insufficiency of linear coding in network information flow. *IEEE Trans. Inform. Theory*, **51**, 2745–2759 (2005).
53. Dougherty, R., Freiling, C. F. & Zeger, K. Unachievability of network coding capacity. *IEEE/ACM Trans. Network.* **14**, 2365–2372 (2006).
54. Huang, R. & Ramamoorthy, A. On the multiple unicast capacity of 3-source, 3-terminal directed acyclic networks. *Information Theory and Applications Workshop (ITA), 2012*, San Diego, CA; DOI:10.1109/ITA.2012.6181808 (2012).
55. Kilin, S. Y. Entangled states and nanoobjects in quantum optics. *Opt. Spectrosc.* **94**, 649–650 (2003).
56. Nevet, A., Hayat, A., Ginzburg, P. & Orenstein, M. Indistinguishable photon pairs from independent true chaotic sources. *Phys. Rev. Lett.* **107**, 253601 (2011).
57. Schröeder, J. Signal processing via Fourier-Bessel series expansion. *Digit. Signal Process.* **3**, 112–124 (1993).

Acknowledgments

This work is supported by the National Natural Science Foundation of China (Nos.61303039, 61272514, 61170272, 61140320, 61121061, 61161140320), Open Foundation of State key Laboratory of Networking and Switching Technology (Beijing University of Posts and Telecommunications)(No.SKLNST-2013-1-11),

NCET(No.NCET-13-0681), the Fok Ying Tong Education Foundation (No.131067), and Science Foundation Ireland (SFI) under the International Strategic Cooperation Award Grant Number SFI/13/ISCA/2845.

Author contributions

L.M.X. proposed the theoretical method. L.M.X. and C.X.B. wrote the main manuscript text. W.X., Y.Y.X. and G.X. reviewed the manuscript.

Additional information

Supplementary information accompanies this paper at http://www.nature.com/scientificreports

Competing financial interests: The authors declare no competing financial interests.

How to cite this article: Luo, M.-X., Xu, G., Chen, X.-B., Yang, Y.-X. & Wang, X.J. Efficient Quantum Transmission in Multiple-Source Networks. *Sci. Rep.* **4**, 4571; DOI:10.1038/srep04571 (2014).

SCIENTIFIC REPORTS

DOI: 10.1038/srep07627

SUBJECT AREAS:
QUANTUM INFORMATION
INFORMATION TECHNOLOGY
QUANTUM OPTICS

SCIENTIFIC REPORTS:
4 : 4571
DOI: 10.1038/srep04571 (4571)

Published:
2 April 2014

Updated:
16 January 2015

RETRACTION: Efficient Quantum Transmission in Multiple-Source Networks

Ming-Xing Luo, Gang Xu, Xiu-Bo Chen, Yi-Xian Yang & Xiaojun Wang

The authors wish to retract this Article because the main improvements reported are invalid.

(1) The paper has not considered how to route quantum information. This is an essential problem in classical network communication such as TCP/IP.

(2) In the presented quantum network, the quantum address or quantum IP address representation for each quantum node has not been designed. In this point of view, different quantum signals going into one common quantum channel cannot be distinguished for their different goal addresses.

(3) The synchronizations of the oscillators are only useful when different quantum signals may be distinguished. From (3), they cannot be completed for quantum network. For an example, see the following figure, there are three incoming edges and three outcoming edges. The synchronizations of the oscillators may be false if the nodes C and D do not know the outcoming paths of three incoming quantum signals. For an example, our synchronizations are shown in Figure 1a while the real paths may be those shown in Figure 1b. Even if one can synchronize them before the transmission, the transmission goals may be different in each time.

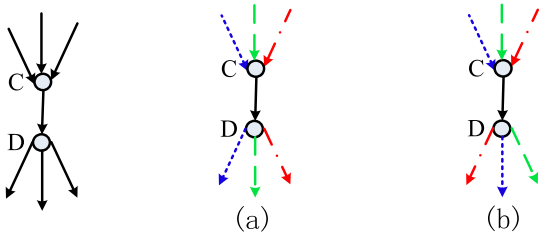

Figure 1 |